New Insight into Photochemistry of Ferrioxalate

Ivan P. Pozdnyakov,* Oksana V. Kel, Victor F. Plyusnin, Vjacheslav P. Grivin, and Nikolai M. Bazhin

Institute of Chemical Kinetics and Combustion, Institutskaya 3, and Novosibirsk State University, Pirogova 2, 630090 Novosibirsk, Russia

Received: May 8, 2008; Revised Manuscript Received: June 20, 2008

Optical spectroscopy and nanosecond flash photolysis (Nd:YAG laser, 355 nm, pulse duration 5 ns, mean energy 5 mJ/pulse) were used to study the photochemistry of $Fe^{III}(C_2O_4)_3^{3-}$ complex in aqueous solutions. The main photochemical process was found to be intramolecular electron transfer from the ligand to Fe(III) ion with formation of a primary radical complex $[(C_2O_4)_2Fe^{II}(C_2O_4^{\bullet})]^{3-}$. The yield of radical species (i.e., $CO_2^{\bullet -}$ and $C_2O_4^{\bullet -}$) was found to be less than 6% of $Fe^{III}(C_2O_4)_3^{3-}$ disappeared after flash. $[(C_2O_4)_2Fe^{II}(C_2O_4^{\bullet})]^{3-}$ dissociates reversibly into oxalate ion and a secondary radical complex, $[(C_2O_4)Fe^{II}(C_2O_4^{\bullet})]^{-}$. The latter reacts with the initial complex and dissociates to $Fe^{II}(C_2O_4)$ and oxalate radical. In this framework, the absorption spectra and rate constants of the reactions of all intermediates were determined.

1. Introduction

The photochemical reactions of Fe(III)−(poly)carboxylate complexes influence many iron-dependent biogeochemical processes and are responsible for photochemical production of CO and CO_2 and for oxygen consumption in natural waters.[1−4] It is assumed that the photolysis of Fe(III)−(poly)carboxylate complexes is one of the main sources of active oxygen species ($^{\bullet}OH$, $HO_2^{\bullet}$, H_2O_2), the formation of which is catalyzed by Fe(II) and Fe(III) ions in Fenton-like reactions.[4−7] Active oxygen species influence the chemical composition and the oxitation−reduction capacity of natural water systems, in particular providing oxidation of sulfur- and nitrogen-containing compounds in the atmosphere.[8,9] However, the primary mechanisms of photoreaction for most Fe(III)−(poly)carboxylate complexes are still not fully investigated.

Among Fe(III)−(poly)carboxylate complexes, the photochemistry of trioxalate Fe(III) complex $[Fe^{III}(C_2O_4)_3^{3-}]$ is of intense interest, as this species not only exhibits high photochemical activity in natural waters under sunlight[8,9] but also is widely used as a stable and sensitive chemical actinometer.[10,11] The total process of $Fe^{III}(C_2O_4)_3^{3-}$ photolysis could be presented as[12]

$$2Fe^{III}(C_2O_2)_3^{3-} \xrightarrow{h\nu} 2Fe^{II}(C_2O_4^{2-})_2^{2-} + 2CO_2 + C_2O_4^{2-} \quad (1.1)$$

The quantum yield of Fe(II) formation in reaction 1.1 is independent of excitation wavelength in the range 270−365 nm and equals 1.24.[10,13] This means that the absorption of UV quantum leads to the photoreduction of the excited complex with a 60% probability.

There are two different points of view on the primary photoprocess following by excitation of $Fe^{III}(C_2O_4)_3^{3-}$: (1) intramolecular electron transfer from the ligand to Fe(III) ion in which the long-lived excited state, the radical complex $[(C_2O_4)_2Fe^{II}(C_2O_4^{\bullet})]^{3-}$ or the $C_2O_4^{\bullet -}$ radical are proposed as primary intermediate(s);[14,15] or (2) sequential cleavage of the Fe(III)−O bond (between one oxalate ligand and Fe(III) ion) and the C−C bond of the ligand, in which biradical complex $[(C_2O_4)_2Fe^{III}(CO_2^{\bullet})_2]^{3-}$ [16] or $CO_2^{\bullet -}$ radical are assumed as primary intermediate(s).[17,18]

In spite of the serious difference of the proposed mechanisms, the successive formation of several (at least two) intermediates is supposed in all aforesaid works. One of these species has an absorption maximum near 400 nm and disappears in the millisecond time range. It was also found that the decay of this intermediate depends on both complex[16−18] and ligand[15,17] concentrations. The $Fe^{II}(C_2O_4)_3^{4-}$ [17] or the $[(C_2O_4)_2Fe^{II}(C_2O_4^{\bullet})]^{3-}$ [14,15] and the $[(C_2O_4)_2Fe^{III}(CO_2^{\bullet})]^{2-}$ [16] radical complexes were assumed as the intermediate with the millisecond lifetime.

Unfortunately, information about the spectral and kinetic properties of primary species formed immediately after excitation of the $Fe^{III}(C_2O_4)_3^{3-}$ complex is rather limited. This is due to the application of methods with insufficient time resolution in the majority of works devoted to the photochemistry of $Fe^{III}(C_2O_4)_3^{3-}$.[14,16,17] So suggestions about the mechanism of $Fe^{III}(C_2O_4)_3^{3-}$ photolysis presented in these works were mainly hypothetical.

There are only two works in which the photochemistry of the $Fe^{III}(C_2O_4)_3^{3-}$ complex was investigated with sufficient time resolution,[15,18] and it is worth noting that the conclusions of these works are in a conflict with each other. In ref 15, two intermediates with lifetimes 30 μs and 1 ms were detected by means of a nanosecond flash photolysis technique. The spectrum of long-lived intermediate corresponds well to transient spectra observed in microsecond flash photolysis experiments.[14,16,17] The short-lived intermediate was assigned to the excited state of the complex ($^*[Fe^{III}(C_2O_4)_3^{3-}]$). This state decays due to electron transfer from ligand to central ion with formation of the long-lived $[(C_2O_4)_2Fe^{II}(C_2O_4^{\bullet})]^{3-}$ radical complex. It was assumed that radical complex dissociates to $Fe^{II}(C_2O_4)_2^{2-}$ and $C_2O_4^{\bullet -}$ radical and oxidation of the latter species by the second $Fe^{III}(C_2O_4)_3^{3-}$ leads to formation of final photoreaction products.

In ref 18, the photochemistry of $Fe^{III}(C_2O_4)_3^{3-}$ was investigated by combination of time-resolved extended X-ray absorption fine structure (EXAFS) spectroscopy, flash photolysis with different time resolution (from femto- to milliseconds), a radical

* Corresponding author: e-mail pozdnyak@kinetics.nsc.ru.

10.1021/jp8040583 CCC: $40.75
Published on Web 08/15/2008

scavenging technique, and theoretical calculations. Ultrafast formation (<2 ps) of an absorption band with a maximum near 430 nm was observed, which was assigned to the excited state of $Fe^{III}(C_2O_4)_3^{3-}$. At 4 and 9 ps after excitation, the length of the Fe−O bond was found to decrease to 1.93 and 1.87 Å, respectively. When it was taken into account that the experimental values of Fe(II)−O bonds are always higher than those of Fe(III)−O, the primary photoprocess was proposed to be Fe−O bond cleavage in the excited state with formation of five-coordinated $[(C_2O_3)O-Fe^{III}(C_2O_4)_2]^{3-}$ intermediate. This process is accompanied by C−C bond cleavage of the ligand, leading to formation of stable $Fe^{III}(C_2O_4)_2^-$ complex and $CO_2^{\bullet -}$ radical:

$$*[Fe^{III}(C_2O_4)_3^{3-}] \rightarrow [(C_2O_3)OFe^{III}(C_2O_4)_2]^{3-} \rightarrow Fe^{III}(C_2O_4)_2^- + 2CO_2^{\bullet -} \quad (1.2)$$

$$*[Fe^{III}(C_2O_4)_3^{3-}] \rightarrow Fe^{III}(C_2O_4)_2^- + 2CO_2^{\bullet -} \quad (1.3)$$

The authors[18] could not distinguish between reactions 1.2 and 1.3 due to insufficient time resolution of EXAFS method. For both $[(C_2O_3)O-Fe^{III}(C_2O_4)_2]^{3-}$ and $Fe^{III}(C_2O_4)_2^-$, theoretical calculations predict a Fe−O bond length of about 1.9 Å. The existence of reactions 1.2 and 1.3 was also supported by more than 50% decrease in Fe(II) quantum yield upon the addition of radical scavenger (thymine) in ferrioxalate solution.

At longer time scales (from tens of nanoseconds to 2 ms), the transient absorption signal exhibits biexponential decay in a similar manner as observed in ref 15. This behavior was explained by the following set of reactions:[18]

$$Fe^{III}(C_2O_4)_2^- + CO_2^{\bullet -} \rightarrow Fe^{II}(C_2O_4)_3^{4-} + CO_2 \quad (1.4)$$

$$Fe^{II}(C_2O_4)_3^{4-} \leftrightarrow Fe^{II}(C_2O_4)_2^{2-} + C_2O_4^{2-} \quad (1.5)$$

The last reaction has to explain dependence of the intermediate absorption decay on a ligand concentration observed in the previous work.[17] So in the mechanism of photoreactions proposed,[18] the main intermediates on the aforementioned time scale are the oxalate complexes of Fe(III) and Fe(II). Both species are supposed to have absorption bands in the near UV, with maxima at 430 nm $[Fe^{III}(C_2O_4)_2^-]$ and 400 nm $[Fe^{II}(C_2O_4)_3^{4-}]$.

Thus, the mechanism of $Fe^{III}(C_2O_4)_3^{3-}$ photolysis is still open to discussion. In this work, a nanosecond flash photolysis technique was used to clarify the nature and the spectral and kinetic properties of transient species formed after excitation of ferrioxalate solution. The main attention was concentrated on (1) reinvestigation of spectroscopy of stable Fe(II) and Fe(III) oxalate complexes; (2) the search for the experimental evidence for organic radical (i.e., $CO_2^{\bullet -}$ and $C_2O_4^{\bullet -}$) formation in the primary photochemical process; and (3) detailed investigation of the kinetics of the intermediates' decay in the wide range of ligand and ferrioxalate concentration.

2. Experimental Details

Laser flash photolysis experiments were performed in a setup with YAG laser excitation (355 nm, pulse duration 5 ns, mean energy 5 mJ/pulse) analogous to that described elsewhere.[19] Absorption spectra were recorded on an HP 8453 Agilent spectrophotometer. For the numerical calculations of kinetic curves, the differential equations were solved by means of the fourth-order Runge−Kutta method. The composition of Fe(II) and Fe(III) complexes was calculated with the Visual MINTEQ 2.32 program.

$K_3Fe(C_2O_4)_3$ (analytical grade) was recrystallized from aqueous solution before use. $K_2C_2O_4$ (analytical grade) and methyl viologen dichloride hydrate (Aldrich, 98%) were used without further purification. Fe(II)−oxalate complexes were obtained by mixing freshly prepared oxygen-free solutions of $FeSO_4$ and $K_2C_2O_4$. $FeSO_4$ solution was obtained by dissolution of carbonyl iron powder (analytical grade) in 0.1 M sulfuric acid (chemical grade) under constant argon bubbling. Fe(II) concentration in the $FeSO_4$ solution was determined by complexometry[12] with 1,10-phenanthroline as a ligand. This method was also used to determine the quantity of Fe(II) produced in the flash experiments.

The samples were prepared with deionized water. Unless otherwise specified, all experiments were carried out with oxygen-free samples at pH = 6−7, ionic strength 0.1 ($LiClO_4$, chemical grade), and 298 K in a 1 cm optical cell. Oxygen was removed by bubbling solutions with gaseous argon. Initial concentrations of $K_3Fe(C_2O_4)_3$ and $K_2C_2O_4$ were varied in the ranges $(1-12) \times 10^{-4}$ and $(3-300) \times 10^{-4}$ M, respectively. Under the aforesaid conditions, the main form (>90%) of Fe(III) in solution was $Fe^{III}(C_2O_4)_3^{3-}$ complex.[20] Samples for flash photolysis were used until a 10% decrease in UV absorption occurred.

3. Results and Discussion

3.1. Optical Spectroscopy of Fe(II) and Fe(III) Oxalate Complexes. Depending on the pH and the concentrations of Fe(III) and oxalate ions, complexes with one, two, and three ligands in the coordination sphere of Fe(III) ion can exist in aqueous solutions:[20]

$$Fe^{3+}_{aq} + C_2O_4^{2-} \leftrightarrow Fe(C_2O_4)^+ \qquad pK_1 = 9.4$$

$$Fe^{3+}_{aq} + 2C_2O_4^{2-} \leftrightarrow Fe(C_2O_4)_2^- \qquad pK_2 = 16.2$$

$$Fe^{3+}_{aq} + 3C_2O_4^{2-} \leftrightarrow Fe(C_2O_4)_3^{3-} \qquad pK_3 = 20.2$$

All Fe(III)−oxalate complexes exhibit charge-transfer (CT) bands with maxima about 260 nm overlapping with a strong absorption band of the ligands at 210 nm.[6,12,18] Intensity of the CT band increases with increasing of number of ligands (Figure 1a).

The main product of $Fe^{III}(C_2O_4)_3^{3-}$ photolysis is $Fe^{II}(C_2O_4)_2^{2-}$. This complex can reversibly dissociate to $Fe^{II}(C_2O_4)$ and free oxalate ion:[21]

$$Fe^{2+}_{aq} + C_2O_4^{2-} \leftrightarrow Fe^{II}(C_2O_4) \qquad pK_1 = 3.05$$

$$Fe^{2+}_{aq} + 2C_2O_4^{2-} \leftrightarrow Fe^{II}(C_2O_4)_2^{2-} \qquad pK_2 = 5.01$$

The spectroscopy of Fe(II)−oxalate complexes is not well described in the literature, so our first step was to obtain information about the absorption spectra of these complexes. At concentration of oxalate ions greater than 3×10^{-3} M, more than 85% of Fe(II) ions are bound in oxalate complexes and the contribution of Fe^{2+}_{aq} to the observed optical spectrum is negligible (Fe^{2+}_{aq} complex absorbs weakly in UV region;[22] $\lambda_{max} = 239$ nm, $\varepsilon^{239} = 20\ M^{-1}\ cm^{-1}$). In this condition one can use an effective absorption coefficient of Fe(II)−oxalate complexes $[\varepsilon(Fe^{II})]$ that is related to absorption coefficients of the individual complexes by

$$\varepsilon_1 + \varepsilon_2 \frac{\alpha_2}{\alpha_1} = \frac{\varepsilon(Fe^{II})}{\alpha_1} \quad (3.1)$$

where α and ε are percentage and absorption coefficients of an individual complex, and indices 1 and 2 correspond to $Fe^{II}(C_2O_4)$ and $Fe^{II}(C_2O_4)_2^{2-}$, respectively.

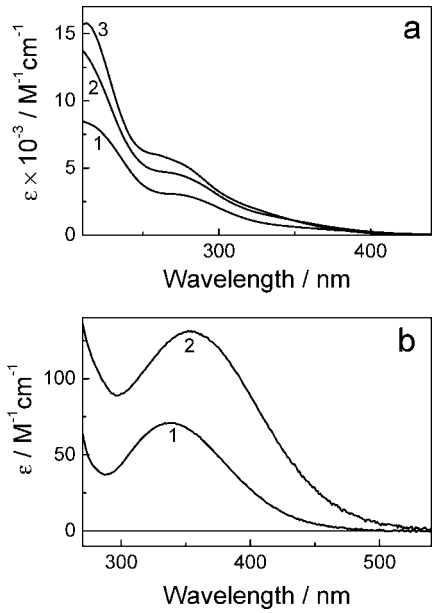

Figure 1. Optical absorption spectra of (a) Fe(III)−oxalate and (b) Fe(II)−oxalate complexes in aqueous solution: (a) (1) $Fe^{III}(C_2O_4)^+$, (2) $Fe^{III}(C_2O_4)_2^-$, and (3) $Fe^{III}(C_2O_4)_3^{3-}$. (b) (1) $Fe^{II}(C_2O_4)$ and (2) $Fe^{II}(C_2O_4)_2^{2-}$.

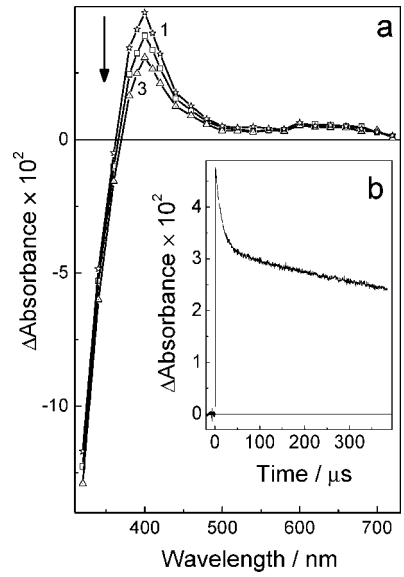

Figure 2. (a) Transient absorption spectra after the excitation at 355 nm of $Fe^{III}(C_2O_4)_3^{3-}$ complex in aqueous solution at pH 7. $[K_3Fe(C_2O_4)_3] = 5 \times 10^{-4}$ M; $[K_2C_2O_4] = 10^{-2}$ M. Spectra 1−3 were taken at 0.05, 10, and 50 μs after the laser flash. (b) Typical kinetic curve at 400 nm.

In Figure 1b, spectra of $Fe^{II}(C_2O_4)$ and $Fe^{II}(C_2O_4)_2^{2-}$ are presented. These spectra were calculated from a set of optical spectra of Fe(II) solutions with different initial concentration of oxalate ions by use of eq 3.1. Both complexes are characterized by low-intensity absorption bands in the near UV with maxima at 340 nm ($\varepsilon = 70$ M^{-1} cm^{-1}) and 350 nm ($\varepsilon = 130$ M^{-1} cm^{-1}) for $Fe^{II}(C_2O_4)$ and $Fe^{II}(C_2O_4)_2^{2-}$, respectively.

It is worth noting that all aforementioned results are in disagreement with theoretical calculations[18] predicting the maxima of absorption bands of $Fe^{III}(C_2O_4)_2^-$ and $Fe^{II}(C_2O_4)_3^{4-}$ at 430 and 400 nm, respectively. The reason is most probably due to neglect of solvation effects and spin orbital coupling in the theoretical calculations.[18] Both factors seem to be taken into account for correct calculation of optical properties of such highly charged complexes of transient metals like oxalate complexes of Fe(II) and Fe(III) in a polar medium.

3.2. Laser Flash Photolysis of $Fe^{III}(C_2O_4^{2-})_3^{3-}$ Complex. Excitation of an oxygen-free aqueous solution of ferrioxalate at 355 nm gives rise to an intermediate absorption consisting of two bands with maxima at 400 and 640 nm (Figure 2a). Negative optical density at $\lambda < 370$ nm indicates the disappearance of the ground-state absorption of $Fe^{III}(C_2O_4)_3^{3-}$ after excitation. The characteristic kinetic curve at 400 nm is shown in Figure 2b. The change of optical density in the whole range of wavelength (320−720 nm) obeys the biexponential law:

$$\Delta A(\lambda) = A_0(\lambda) + A_1(\lambda)\exp(-k_{fast}t) + A_2(\lambda)\exp(-k_{slow}t) \quad (3.2)$$

where $A_0 = 2[\varepsilon(Fe^{III}) - \varepsilon(Fe^{II})]\Delta[Fe^{III}]$ is the steady-state change of absorbance of ferrioxalate solution (reaction 1.1), $\varepsilon(Fe^{III})$ is the absorption coefficient of $Fe^{III}(C_2O_4)_3^{3-}$, and $\varepsilon(Fe^{II})$ is the effective absorption coefficient of Fe(II)−oxalate complexes.

This fact supports the supposition that excitation of $Fe^{III}(C_2O_4)_3^{3-}$ leads to successive formation of two intermediates absorbing in the near UV.[14−18] The observed rate constants k_{fast} and k_{slow} are independent of a registration wavelength, which indicates that only (pseudo)monomolecular reactions take place in the system. The characteristic lifetimes of the intermediates are 20 μs and 1 ms, which coincide very well with the published data (30 μs and 1 ms).[15]

But does the intermediate with absorption maximum at 400 nm appear to be the single primary species, or does this intermediate appear together with organic radicals $CO_2^{\bullet -}$/$C_2O_4^{\bullet -}$, which absorb at $\lambda < 300$ nm[23,24] and cannot be detected directly in our setup? For detection of organic radicals in our flash experiments, the well-known electron acceptor methyl viologen dication (MV^{2+}) was used.[25,26] This species reacts with both $CO_2^{\bullet -}$ ($k = 1 \times 10^{10}$ M^{-1} s^{-1}) and $C_2O_4^{\bullet -}$ ($k = 4.3 \times 10^9$ M^{-1} s^{-1}) radicals with high rate constants.[24] As a result of the reactions, the cation radical $MV^{\bullet +}$ was formed, which exhibits strong absorption bands at 396 ($\varepsilon = 41\,500$ M^{-1} cm^{-1}) and 605 nm.[27]

Addition of MV^{2+} to solutions containing $Fe^{III}(C_2O_4)_3^{3-}$ leads to formation and decay of an additional transient absorption signal at 396 nm (Figure 3) after complex excitation. The observed rate constant of signal formation depends linearly on MV^{2+} concentration (Figure 3, inset), indicating the formation of $MV^{\bullet +}$ radical cation. The value of the bimolecular rate constant of $MV^{\bullet +}$ formation calculated from the slope ($k_{MV} \approx 1.2 \times 10^{10}$ M^{-1} s^{-1}) is close to the value of the rate constant of the reaction of $CO_2^{\bullet -}$ radical with MV^{2+}.[24] The nonzero value of the intercept of the plot in the inset of Figure 3 corresponds to reaction of the organic radical with $Fe^{III}(C_2O_4)_3^{3-}$. The value of the bimolecular rate constant calculated from the intercept ($k_{Fe} \approx 5.5 \times 10^9$ M^{-1} s^{-1}) is also close to the value of the rate constant for the reaction of $CO_2^{\bullet -}$ radical with the complex.[28] So one can assume that $MV^{\bullet +}$ radical cation is formed in the reaction of MV^{2+} with $CO_2^{\bullet -}$ radical.

In the absence of dissolved oxygen and other possible oxidizers, the concentration of $MV^{\bullet +}$ practically does not change during several minutes.[29] In our case, the decay of $MV^{\bullet +}$ (Figure 3) seems to be determined by the reaction with $Fe^{III}(C_2O_4)_3^{3-}$ complex.

The initial concentration of $CO_2^{\bullet -}$ could be directly calculated from the concentration of $MV^{\bullet +}$ under conditions when all organic radicals are quenched by MV^{2+}. At $[MV^{2+}] = 10^{-3}$ M, the formation time of $MV^{\bullet +}$ is less than 100 ns, and so the

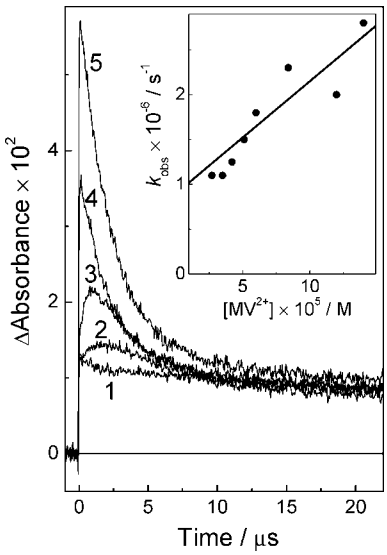

Figure 3. Laser flash photolysis of $Fe^{III}(C_2O_4)_3^{3-}$ (1.6×10^{-4} M) in the presence of MV^{2+}. Curves 1−5 are kinetic curves (396 nm) at initial concentrations of $[MV^{2+}] \times 10^5 = 0$, 2.7, 8.4, 25, and 100 M, respectively. (Inset) Dependence of the observed rate constant (k_{obs}^{396}) of $MV^{\bullet+}$ formation on MV^{2+} concentration.

concentration of $MV^{\bullet+}$ (and $CO_2^{\bullet-}$) is easily calculated from the difference in the initial amplitudes of the signals at 400 nm, corresponding to kinetic curves 5 and 1 in Figure 3. One can estimate that the yield of $CO_2^{\bullet-}$ (ca. 1.2×10^{-6} M) is less than 6% of the number of $Fe^{III}(C_2O_4)_3^{3-}$ complexes photolyzed (ca. 2×10^{-5} M). This result is in contradiction with indirect radical-scavenging experiments.[18] The large (more than 50%) decrease of Fe(II) quantum yield was observed after the addition of thymine in ferrioxalate solution, which was interpreted by scavenging of $CO_2^{\bullet-}$ radical formed in reactions 1.2 and 1.3 by thymine. Most probably the results[18] should be explained by oxidation of final Fe(II)−oxalate complexes or the transient species by thymine rather than by reaction of $CO_2^{\bullet-}$ radical with the scavenger.

Thus, the species with absorption maximum at 400 nm is the main primary intermediate arising upon $Fe^{III}(C_2O_4)_3^{3-}$ photolysis. By carrying out a parallel determination of the transient absorption signal at 400 nm and the concentration of Fe(II) ions, one can calculate the absorption coefficient of this species at 400 nm ($\varepsilon \approx 780$ M^{-1} cm^{-1}). It is worth noting that the variation of MV^{2+} concentration has no effect on the lifetime of the intermediate absorbing at 400 nm (Figure 3), indicating the absence of reaction between these species.

3.3. Nature of Primary Intermediate in Photochemistry of $Fe^{III}(C_2O_4)_3^{3-}$. As was mentioned in the Introduction, several species are candidates for the role of primary intermediate absorbing at 400 nm: (1) the $Fe^{III}(C_2O_4)_2^-$ complex, (2) the long-lived excited state of $Fe^{III}(C_2O_4)_3^{3-}$, (3) the biradical complex $[(C_2O_4)_2Fe^{III}(CO_2^{\bullet})_2]^{3-}$, and (4) the $[(C_2O_4)_2Fe^{II}(C_2O_4^{\bullet})]^{3-}$ radical complex (hereafter in the text referred to as RC1).

As was shown in section 3.1, the $Fe^{III}(C_2O_4)_2^-$ complex does not have an absorption band with a maximum at 400 nm, and the absorption coefficient of this complex at this wavelength (270 M^{-1} cm^{-1}) is much less than the calculated one for the primary intermediate (780 M^{-1} cm^{-1}). Also, the formation of $Fe^{III}(C_2O_4)_2^-$ has to be accompanied by formation of $CO_2^{\bullet-}$ radical. As the yield of the latter species was found to be negligible, the formation of $Fe^{III}(C_2O_4)_2^-$ in the photolysis of $Fe^{III}(C_2O_4)_3^{3-}$ must be ruled out.

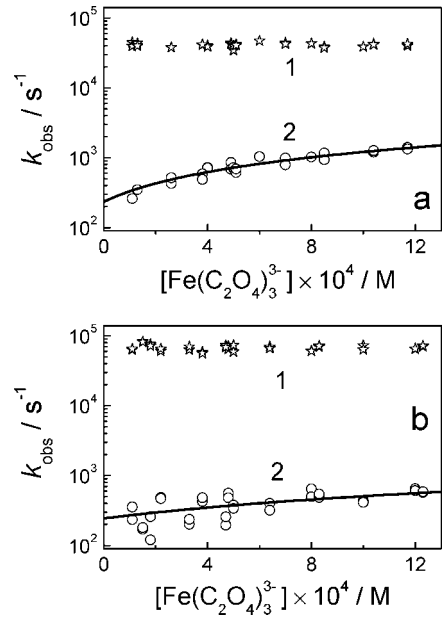

Figure 4. Dependence of the observed rate constants (1) k_{fast} and (2) k_{slow} on the concentration of $Fe^{III}(C_2O_4)_3^{3-}$ at initial free oxalate ion concentrations of (a) 10^{-3} M and (b) 10^{-2} M. Curves are linear approximations of the experimental data (note that the *y*-axis has a logarithmic scale).

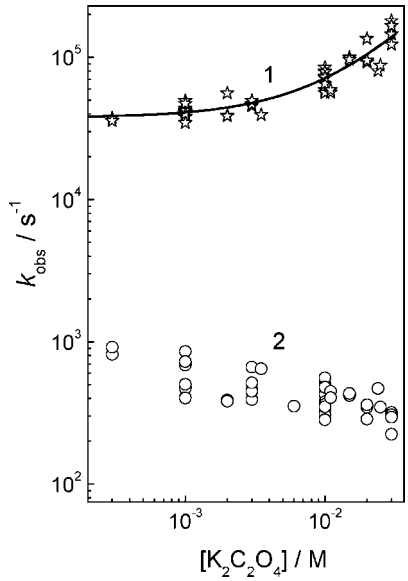

Figure 5. Dependence of the observed rate constants (1) k_{fast} and (2) k_{slow} on the concentration of free oxalate ions. The curve is a linear approximation of the experimental data (note that both axes have logarithmic scales).

To distinguish between candidates 2−4, the dependence of k_{fast} on the pH and initial concentration of oxygen, ferrioxalate, and oxalate ions was investigated in detail. It was observed that k_{fast} is independent of pH in the range 5.5−7.5 (similar to published data[15,16]), concentration of oxygen (data not shown), and ferrioxalate (Figure 4a,b) and increases linearly with increasing concentration of free ligand (Figure 5). It is worth noting that the increase of $C_2O_4^{2-}$ concentration has no effect on initial amplitude of the transient signal at 400 nm but leads to increased absorbance of the long-lived species (Figure 6a).

The absence of quenching of the primary intermediate by $Fe^{III}(C_2O_4)_3^{3-}$, oxygen, and MV^{2+} means that the primary species is not the long-lived excited state of $Fe^{III}(C_2O_4)_3^{3-}$. The

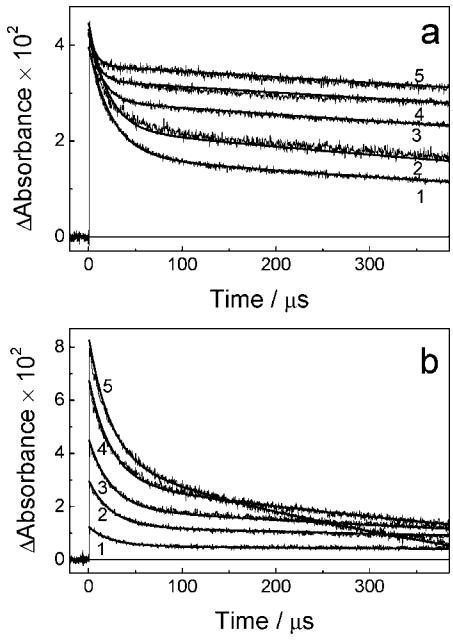

Figure 6. (a) Kinetic curves at 400 nm. (Curves 1−5) $[K_2C_2O_4] \times 10^3 = 1$, 3, 10, 20, and 30 M, respectively; $[K_3Fe(C_2O_4)_3] = 5 \times 10^{-4}$ M. (b) Kinetic curves at 400 nm. (Curves 1−5) $[K_3Fe(C_2O_4)_3] \times 10^4 = 1.3$, 2.6, 5.1, 8.5, and 16.4 M, respectively; $[K_2C_2O_4] = 10^{-3}$ M. The smooth curves are fits by numeric solutions of the system of the differential equations corresponding to eqs 3.3−3.8, with the average values of the parameters listed in Table 1.

formation of this state was based on flash experiments[15] in which the decreased lifetime of the primary species with increased ferrioxalate concentration was observed. This fact was interpreted as self-quenching of the excited state of $Fe^{III}(C_2O_4)_3^{3-}$ by the initial complex. However, the lifetime of primary intermediate was measured at a constant [Fe(III)]/[oxalate] ratio, that is, with a synchronous increase in both complex and ligand concentrations.[15] So one can conclude that the results[15] are well explained by the increase of k_{fast} (which is a reverse lifetime of primary species) with increasing ligand concentration (Figure 5). Moreover, the lifetime of $*[Fe(C_2O_4)_3^{3-}]$ (ca. 30 μs)[15] is 1−2 orders of magnitude higher than the typical lifetimes of the excited states of the metal complexes.[30]

The independence of k_{fast} from the concentration of oxygen and MV^{2+} also conflicts with the hypothesis that the $[(C_2O_4)_2Fe^{III}(CO_2^{\bullet})_2]^{3-}$ biradical complex is formed in a primary photochemical process, because $CO_2^{\bullet -}$ radical reacts with both species.[24] The fast intramolecular electron transfer from coordinated $CO_2^{\bullet -}$ on the central Fe(III) ion could also be expected. Moreover, dependence of k_{fast} on $[C_2O_4^{2-}]$ cannot be explain in the framework of hypothesis of $[(C_2O_4)_2Fe^{III}(CO_2^{\bullet})_2]^{3-}$ formation.

Thus, radical complex RC1 is the most probable candidate for the role of the primary intermediate. It worth noting that formation of radical complexes is a typical feature of photochemistry of transient metals and is shown for the number of coordination compounds of copper, chromium, manganese, cobalt, nickel, and platinum.[31,32] Unfortunately, our time resolution is not sufficient to determine the precursor of RC1. It could be the primary excited state populated upon a ligand-to-metal charge transfer- (LMCT-) type transition or a long-lived secondary excited state (so-called THEXI state) populated after relaxation of the LMCT state.[30] One piece of evidence for THEXI state formation is independence (or weak dependence) of the quantum yield of photolysis on excitation wavelength. As the quantum yield of $Fe^{III}(C_2O_4)_3^{3-}$ photolysis depends weakly on excitation wavelength,[11] we can tentatively assume that a THEXI state is a precursor of RC1.

Below, interpretation of all experimental results in the framework of RC1 formation at $Fe^{III}(C_2O_4)_3^{3-}$ excitation is presented.

3.4. Kinetic Scheme of $Fe^{III}(C_2O_4)_3^{3-}$ Photolysis. To explain the observed dependence of k_{fast} on the concentration of oxalate ions, the reversible dissociation of RC1 from the secondary $[(C_2O_4)Fe^{II}(C_2O_4^{\bullet})]^-$ radical complex (hereafter in the text known as RC2) and oxalate ion was proposed:

$$RC1 \xrightarrow{k_1} RC2 + C_2O_4^{2-} \quad (3.3)$$

$$RC2 + C_2O_4^{2-} \xrightarrow{k_2} RC1 \quad (3.4)$$

This supposition is based on the smaller stability of Fe(II)−oxalate complexes compared with Fe(III)−oxalate complexes.[20,21] One can estimate the values of the rate constants k_1 ($\approx 3.8 \times 10^4$ s^{-1}) and k_2 ($\approx 3.4 \times 10^6$ M^{-1} s^{-1}) from the linear fitting of dependence of k_{fast} on the concentration of oxalate ions (Figure 5).

k_{slow} decreases with increasing ligand concentration (Figure 5, in agreement with published results[17]) and rises linearly with increasing ferrioxalate concentration (Figure 4a,b). The slope ratio of dependence of k_{slow} on $[Fe^{III}(C_2O_4)_3^{3-}]$ decreases with increasing ligand concentration (Figure 4a,b), indicating that only RC2 reacts with the initial complex:

$$RC2 + Fe^{III}(C_2O_4)_3^{3-} \xrightarrow{k_3} 2Fe^{II}(C_2O_4)_2^{2-} + 2CO_2 \quad (3.5)$$

Most probably, that reaction between RC1 and $Fe^{III}(C_2O_4)_3^{3-}$ is very slow and is not observed under our experimental conditions due to strong Coulomb repulsion (both complexes have a high negative charge, $q = -3$).

The value of the rate constant k_3 ($\geq 9 \times 10^5$ M^{-1} s^{-1}) could be estimated from the slope ratio of dependence of k_{slow} on $[Fe^{III}(C_2O_4)_3^{3-}]$ at low ligand concentration (Figure 4a). The low value of k_3 is explained by negative charges of both reagents. The nonzero value of the intercepts of the plots in Figure 4a,b corresponds to the monomolecular dissociation of both radical complexes with approximately the same rate constants ($k_4 \approx k_5 \approx 150$ M^{-1} s^{-1}):

$$RC2 \xrightarrow{k_4} Fe^{II}(C_2O_4) + C_2O_4^{\bullet -} \quad (3.6)$$

$$RC1 \xrightarrow{k_5} Fe^{II}(C_2O_4)_2^{2-} + C_2O_4^{\bullet -} \quad (3.7)$$

Oxalate radical formed in reactions 3.6 and 3.7 reacts most probably with the initial complex:

$$C_2O_4^{\bullet -} + Fe^{III}(C_2O_4)_3^{3-} \xrightarrow{k_6} Fe^{II}(C_2O_4)_2^{2-} + C_2O_4^{2-} + 2CO_2 \quad (3.8)$$

The rate constant of reaction 3.8 cannot be determined directly, as oxalate radical exhibits an absorption band in a wavelength region unregistered by our setup ($\lambda < 300$ nm[24]). We propose that the value of k_6 is close to value of the rate constant of the reaction of $CO_2^{\bullet -}$ radical with $Fe^{III}(C_2O_4)_3^{3-}$ and exceeds

TABLE 1: Parameters Used in Numerical Simulation of Kinetic Curves at 400 nm

$\varepsilon(Fe^{III})$, M^{-1} cm^{-1}	ε(RC1), M^{-1} cm^{-1}	ε(RC2), M^{-1} cm^{-1}	$k_1 \times 10^{-4}$, s^{-1}	$k_2 \times 10^{-6}$, M^{-1} s^{-1}	$k_3 \times 10^{-6}$, M^{-1} s^{-1}	$k_4 \times 10^{-2}$, s^{-1}	$k_5 \times 10^{-2}$, s^{-1}
140[a]	780[a]	370 ± 30	3.8[a]	3.4[a]	1.1 ± 0.2	1.7 ± 0.7	1.6 ± 0.7

[a] Fixed parameter.

10^9 M^{-1} s^{-1}. This assumption is based on proximity of the values of the rate constants for reactions of both radicals with MV^{2+}. As the decay rate of the oxalate radical in reaction 3.8 ($k_6[Fe^{III}(C_2O_4)_3]^{3-} > 5 \times 10^5$ s^{-1}) exceeds greatly its generation rate in reactions 3.6 and 3.7 ($k_4 + k_5 < 500$ s^{-1}), one can use the method of stationary concentrations with reference to this intermediate.

3.5. Simulation of Experimental Kinetic Curves at 400 nm. If $d[C_2O_4^{\bullet -}]/dt = 0$ and fast equilibrium between Fe(II)−oxalate complexes takes place, one can express the change in concentrations of the reagents and intermediates by the following set of differential equations:

$$\frac{d[RC1]}{dt} = -(k_1 + k_5)[RC1] + k_2'[RC2]$$

$$\frac{d[RC2]}{dt} = k_1[RC1] - (k_2' + k_3')[RC2]$$

$$\frac{d[Fe(III)]}{dt} = -k_5[RC1] - k_3'[RC2]$$

$$\frac{d[Fe(II)]}{dt} = 2k_5[RC1] + 2k_3'[RC2] \qquad (3.9)$$

where [Fe(III)] and [Fe(II)] describe the change in concentrations of $Fe^{III}(C_2O_4)_3^{3-}$ and Fe(II)−oxalate complexes, respectively; $k_2' = k_2[C_2O_4^{2-}]$, and $k_3' = k_3[Fe^{III}(C_2O_4)_3^{3-}] + k_4$.

The system of differential equations (eq 3.9) can be solved analytically on the assumption that both $[C_2O_4^{2-}]$ and $[Fe^{III}(C_2O_4)_3^{3-}] \gg$ [RC1]. This assumption works well at $[C_2O_4^{2-}] > 5 \times 10^{-4}$ M and low intensity of excitation, when less than 20% of initial complexes are decomposed in irradiated volume. The analytical solution of the system (eq 3.9) for change of optical density at 400 nm gives an expression absolutely identical with eq 3.2, where

$$k_{fast} = k_1 + k_2[C_2O_4^{2-}] + k_3[Fe^{III}(C_2O_4)_3^{3-}] + k_4 + k_5$$

$$k_{slow} = (k_3[Fe^{III}(C_2O_4)_3^{3-}] + k_4)\{k_1/(k_1 + k_2[C_2O_4^{2-}])\}$$

Components A_1 and A_2 (eq 3.2) are complex functions of the absorption coefficients of initial, radical, and final complexes and the rate constants of reactions (3.3−3.8). It is very important that the analytical expressions of k_{fast} and k_{slow} by the rate constants of elementary stages fully coincide with our experimental data (Figures 4 and 5). k_{fast} exhibits linear dependence on ligand concentration and is independent of ferrioxalate concentration because in our conditions $k_3[Fe^{III}(C_2O_4)_3^{3-}] < 1500$ $s^{-1} \ll k_1 = 3.8 \times 10^4$ s^{-1}. k_{slow} exhibits linear dependence on ferrioxalate concentration and is inversely proportional to ligand concentration.

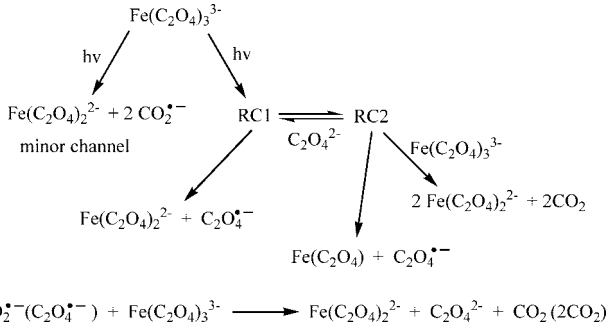

Figure 7. General scheme of $Fe^{III}(C_2O_4)_3^{3-}$ photolysis.

To obtain more accurate values of rate constants (eqs 3.3−3.8) and to determine the absorption coefficient of RC2, all experimental kinetic curves at 400 nm were fitted by numerical solutions of the system of differential equations (eq 3.9) by the fourth-order Runge−Kutta method. As fixed parameters, the absorption coefficients of $Fe^{III}(C_2O_4)_3^{3-}$ and RC1 [$\varepsilon(Fe^{III})$ and ε_{RC1}] and rate constants of reversible dissociation of RC1 (k_1 and k_2) were used. As variable parameters, the absorption coefficient of RC2 (ε_{RC2}) and the rate constants of disappearance of RC1 and RC2 (k_3, k_4, and k_5) were used. Dependence of $\varepsilon(Fe^{II})$ on oxalate ion concentration was also taken into account, although this parameter has a weak influence on results of fitting.

The results of fitting of about 90 experimental kinetic curves [with different initial concentrations of oxalate ions, $Fe^{III}(C_2O_4)_3^{3-}$, and RC1] are summarized in Table 1. The smooth lines in Figure 6 show calculations with the average values of parameters presented in Table 1. Full agreement between calculated and experimental curves was observed over a wide range of concentrations of reagents and at the same time with values of variable parameters close to the experimental one (Table 1). These facts allow us to maintain the adequacy of the proposed mechanism of the photolysis of $[Fe^{III}(C_2O_4)_3]^{3-}$ complex (Figure 7).

Information about rate constants (eqs 3.3−3.8) allows one to calculate the absorption spectra of the radical complexes. Figure 8a presents the results of global fitting of experimental kinetic curves in the range 300−520 nm to eq 3.2. The best agreement of the calculated and experimental kinetic curves was

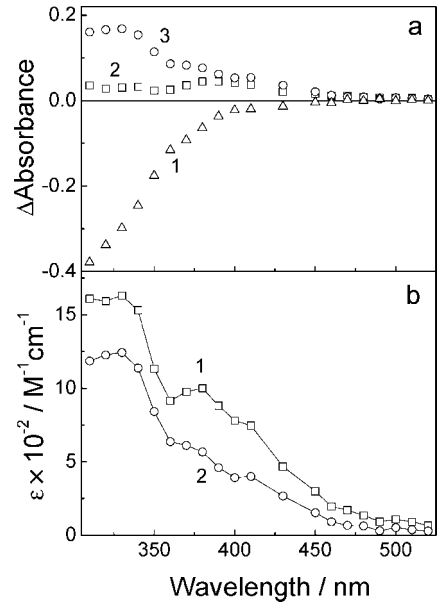

Figure 8. (a) Spectra of (1) $A_0(\lambda)$, (2) $A_1(\lambda)$, and (3) $A_2(\lambda)$ components (eq 3.2), corresponding to $k_{fast} = 4.5 \times 10^4$ s^{-1} and $k_{slow} = 670$ s^{-1}. (b) Calculated absorption spectra of (1) RC1 and (2) RC2. $[K_3Fe(C_2O_4)_3] = 5 \times 10^{-4}$ M; $[K_2C_2O_4] = 10^{-3}$ M.

obtained at $k_{fast}(fit) = 4.5 \times 10^4\ s^{-1}$ and $k_{slow}(fit) = 670\ s^{-1}$. These values are in fair agreement with the calculated ones from data in Table 1 [$k_{fast}(calc) = 4.2 \times 10^4\ s^{-1}$ and $k_{slow}(calc) = 650\ s^{-1}$]. At the ligand concentration used (10^{-3} M), the sum of amplitudes A_1 and A_2 corresponds to the absorption spectrum of RC1 and amplitude A_2 corresponds to the absorption spectrum of RC2. The calculated absorption spectra of radical complexes are presented in Figure 8b. Both radical complexes exhibit absorption bands with maxima at 330 and 380 nm. It is worth noting that stable Fe(II)−oxalate complexes have absorption bands in the same region (Figure 1b). The intensity of the absorption bands of the radical complexes decreases with decreasing coordination number, which is typical for spectroscopy of the stable Fe(II)− and Fe(III)−oxalate complexes (Figure 1a,b).

4. Conclusions

Laser flash photolysis experiments carried out with a wide range of initial parameters provide new evidence that intramolecular electron transfer from ligand to Fe(III) ion is a main photochemical process in $Fe^{III}(C_2O_4)_3^{3-}$ photochemistry. As primary intermediate, the radical complex $(C_2O_4)_2Fe^{II}(C_2O_4^{\bullet})^{3-}$ is formed; the yield of organic radicals in the primary photoprocess is negligible.

A kinetic scheme for $Fe^{III}(C_2O_4)_3^{3-}$ photolysis was proposed, including formation of $(C_2O_4)_2Fe^{II}(C_2O_4^{\bullet})^{3-}$, its reversible dissociation to the oxalate ion and secondary radical complex $(C_2O_4)Fe^{II}(C_2O_4^{\bullet})^{-}$, and the decay of both radical complexes. In the framework of this scheme, the absorption spectra and rate constants of formation and decay of all intermediates were determined.

Acknowledgment. This work was supported by RFBR (Grants 06-03-110, 06-03-32110, 05-03-39007GFEN, 08-03-90102-Mol, and 08-03-00313) and by Program of Integration projects of SB RAS-2006 (Grant 4.16).

References and Notes

(1) Miles, C. J.; Brezonik, P. L. *Environ. Sci. Technol.* **1981**, *15*, 1089.
(2) Zuo, Y.; Jones, R. D. *Water Res.* **1997**, *31*, 850.
(3) Voelker, B. F.; Morel, M. M.; Sulzberger, B. *Environ. Sci. Technol.* **1997**, *31*, 1004.
(4) Gao, H.; Zepp, R. G. *Environ. Sci. Technol.* **1998**, *32*, 2940.
(5) Behra, P.; Sigg, L. *Nature* **1990**, *344*, 419.
(6) Zuo, Y.; Holdne, J. *Environ. Sci. Technol.* **1992**, *26*, 1014.
(7) Faust, B. S.; Zepp, R. G. *Environ. Sci. Technol.* **1993**, *27*, 2517.
(8) Zuo, Y.; Zhan, J. *Atmos. Environ.* **2005**, *39*, 27.
(9) Zuo, Y.; Hoigne, J. *Science.* **1993**, *260*, 71.
(10) Calvert, J.; Pitts J. N. *Photochemistry*; John Wiley and Sons: New York, London, and Sydney, 1967.
(11) Kurien, K. C. *J. Chem. Soc. B* **1971**, 2081.
(12) Balzani, V.; Carassiti, V. *Photochemistry of Coordination Compounds*; Academic Press: London and New York, 1970.
(13) Goldstein, S.; Rabani, J. *J. Photochem. Photobiol., A* **2008**, *193*, 50.
(14) Parker, C. A.; Hatchard, C. G. *Nature* **1955**, *176*, 122.
(15) Nadtochenko, V.; Kiwi, J. *J. Photochem. Photobiol., A* **1996**, *99*, 145.
(16) Patterson, J. I. H.; Perone, S. P. *J. Phys. Chem.* **1973**, *77*, 2437.
(17) Cooper, G. D.; DeGraff, B. A. *J. Phys. Chem.* **1971**, *75*, 2897.
(18) Chen, J.; Zhang, H.; Tomov, I. V.; Wolfsberg, M.; Ding, X.; Rentzepis, P. M. *J. Phys. Chem. A* **2007**, *111*, 9326.
(19) Pozdnyakov, I. P.; Plyusnin, V. F.; Grivin, V. P.; Vorobyev, D. Yu.; Bazhin, N. M.; Vauthey, E. *J. Photochem. Photobiol., A* **2006**, *182*, 75.
(20) Sillen, L. G.; Martell, A. E. *Stability constants of metal-ion complexes*; The Chemical Society: London, 1964.
(21) Micskei, K. *J. Chem. Soc., Dalton. Trans.* **1987**, 255.
(22) Jortnor, J.; Stein, G. *J. Phys. Chem.* **1962**, *66*, 1264.
(23) Neta, P.; Simic, M.; Hayon, E. *J. Phys. Chem.* **1969**, *73*, 4207.
(24) Mulazzani, Q. G.; D'Angelantonio, M.; Venturi, M.; Hoffman, M. Z.; Rodgers, M. A. J. *J. Phys. Chem.* **1986**, *90*, 5347.
(25) Feng, W.; Nansheng, D.; Glebov, E. M.; Pozdnyakov, I. P.; Grivin, V. P.; Plyusnin, V. F.; Bazhin, N. M. *Russ. Chem. Bull., Int. Ed.* **2007**, *56*, 900.
(26) Togashi, D. M.; Costa, S. M. B. *Phys. Chem. Chem. Phys.* **2002**, *4*, 1150.
(27) Mulazzani, Q. G.; Venturi, M.; Hoffman, M. Z. *J. Phys. Chem.* **1985**, *89*, 722.
(28) Hislop, K. A.; Bolton, J. R. *Environ. Sci. Technol.* **1999**, *33*, 3119.
(29) Patterson, L.; Small, R.; Scaiano, J. *Radiat. Res.* **1977**, *72*, 218.
(30) Vlcek, A., Jr. *Coord. Chem. Rev.* **2000**, *200−202*, 933.
(31) Muller, J.; Kikuchi, A.; Bill, E.; Weyhermuller, T.; Hildebrandt, P.; Ould-Moussa, L.; Wieghardt, K. *Inorg. Chim. Acta* **2000**, *297*, 265.
(32) Ivanov, Y. V.; Plyusnin, V. F.; Grivin, V. P.; Larionov, S. V. *Chem. Phys. Lett.* **1999**, *310*, 252.

JP8040583